

Neuroadaptive Combined Lateral and Longitudinal Control of Vehicles for IVHS

Sisil Kumarawadu and Tsu-Tian Lee
 Department of Electrical and Control Engineering
 National Chiao-Tung University
 1001 University Road, Hsinchu, Taiwan, 300
 E-mail: sisilkuma@ieee.org, ttlee@cn.nctu.edu.tw

Abstract—A model-based neurocontrol approach for combined lateral and longitudinal control of vehicles for Intelligent Vehicle Highway Systems (IVHS) is presented. The controller is synthesized using a Proportional plus Derivative control coupled with an online adaptive neural module that acts as a dynamic compensator to counteract for inherent model discrepancies, strong nonlinearities and coupling effects. The controller is tested and verified via computer simulations.

I. INTRODUCTION

The problems of lateral control and longitudinal control have been investigated as separate problems in the vast majority of research on control for automated vehicle operation [1]–[3]. It is known, however, that the vehicle dynamics is not independent in both directions. The coupling effects become increasingly significant as maneuvers involve higher accelerations, larger tyre forces, or reduced road friction [7]. Thus, several methods have been proposed to merge the two control tasks into a single problem [4]–[6]. Sliding-mode-control (SMC) has been widely used [2]–[5]. SMC has its major inherent problem in control chatter caused by the switching term in the control law. Robust adaptive control by backstepping has been adopted in [6]. Most importantly, the yaw dynamics has been taken into account. But, simulation tests have been confined to very low operating speeds.

For high-performance control of a mechanical system in terms of accuracy, stability, and robustness, it is of paramount importance to consider its mechanical structures, torques and forces acting upon it. Therefore, it is necessary to have accurate dynamic models of the controlled system, and controllers should be synthesized on the basis of modelled dynamics. On the other hand, the dynamics of vehicle systems are apparently of highly complex nature and are difficult to be modelled accurately. Hence, the controllers should also be able to online adapt to varying conditions and environments, and to efficiently compensate for modelled and unmodelled uncertainties, strong nonlinearities and coupling effects.

A control approach blending the neural networks (NNs) techniques with classical model-based control is presented for combined lateral and longitudinal control for IVHS applications. The neural module is designed to compensate

for model discrepancies and strong coupling effects due to lateral and yaw motions. Weights are tuned completely online with no learning phase needed, and stability is guaranteed using a Lyapunov approach. Complex 3-DOF dynamic model, in the sensor space, is derived for the *Sevrin* (Mitsubishi Motors–Taiwan) passenger wagon, which is used for real world testing at the ITS Center, National Chiao-Tung Univ., Taiwan. Controller design is based on a simplified model that is obtained using small angle approximation to the original model. Simulations are performed in the presence of severe accelerations and model uncertainties using the original complex model.

II. VEHICLE DYNAMICS

The vehicle system used in the analysis is *Sevrin* (Mitsubishi Motors–Taiwan) passenger wagon, which is a FWD/FWS system with 100/0 brake torque distribution as shown in Fig. 1.

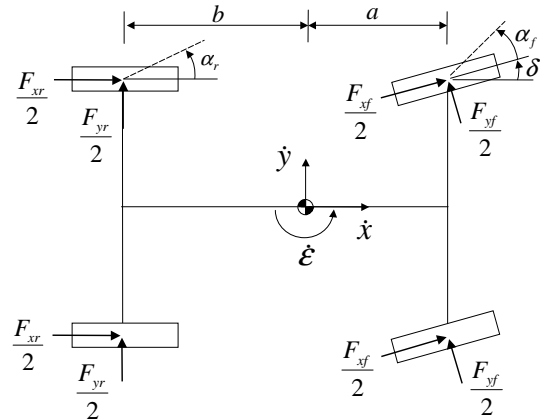


Fig. 1. Vehicle model.

The equations of motion are

$$m\ddot{x} = F_{xr} + F_{xf} \cos \delta - F_{yf} \sin \delta + m\dot{y} - k_D \dot{x}^2 \quad (1)$$

$$m\ddot{y} = F_{yr} + F_{xf} \sin \delta + F_{yf} \cos \delta - m\dot{x} \quad (2)$$

$$I_z \ddot{\epsilon} = aF_{xf} \sin \delta + aF_{yf} \cos \delta - bF_{yr} \quad (3)$$

where \dot{x} , \dot{y} , and $\dot{\epsilon}$ respectively are longitudinal velocity, lateral velocity, and yaw rate. F_{xf} and F_{xr} are longitudinal

forces on front and rear wheels, and F_{yf} and F_{yr} are tire lateral forces. δ is the steering angle. Please refer Table 1 for complete terminology.

Assuming equal slip angles on the left and right wheels, the front and rear slip angles can be approximated as

$$\alpha_f = \frac{\dot{y} + a\dot{\epsilon}}{\dot{x}} - \delta, \quad \alpha_r = \frac{\dot{y} - b\dot{\epsilon}}{\dot{x}}. \quad (4)$$

Using a linear tire model, lateral forces are obtained as

$$F_{yf} = -C_f\alpha_f, \quad F_{yr} = -C_r\alpha_r \quad (5)$$

where C_f and C_r respectively are the front and rear cornering stiffnesses. Tire longitudinal forces F_{xf} and F_{xr} can be written as

$$F_{xf} = F - f\frac{b}{a+b}(mg - k_L\dot{x}^2) \quad (6)$$

$$F_{xr} = -f\frac{a}{a+b}(mg - k_L\dot{x}^2) \quad (7)$$

where F is the net force exerted on the wheels, i.e., $F_{traction} - F_{braking}$.

A simplified model with small angle approximation is used in the controller design. Using small angle approximation, $\cos\delta \approx 1$ and $\sin\delta \approx \delta$, (1) through (3) are rewritten as

$$M\ddot{\mathbf{q}} = \mathbf{h}(\dot{\mathbf{q}}) + \mathbf{g}(\dot{\mathbf{q}}, \mathbf{u}) \quad (8)$$

where $\dot{\mathbf{q}} = [\dot{x} \ \dot{y} \ \dot{\epsilon}]^T$, and $\mathbf{u} = [F \ \delta]^T$ is the vector of control inputs. M is the positive definite mass matrix, and $\mathbf{h}(\dot{\mathbf{q}})$ and $\mathbf{g}(\dot{\mathbf{q}}, \mathbf{u})$ are defined separating the terms that contain control inputs from the rest, as follows

$$M = \text{diag}\left(m, m, \frac{I_z}{a}\right) \quad (9)$$

$$\mathbf{h}(\dot{\mathbf{q}}) = \begin{bmatrix} m\dot{y}\dot{\epsilon} - f(mg - k_L\dot{x}^2) - k_D\dot{x}^2 \\ -m\dot{x}\dot{\epsilon} - C_r\left(\frac{\dot{y}-b\dot{\epsilon}}{\dot{x}}\right) - C_f\left(\frac{\dot{y}+a\dot{\epsilon}}{\dot{x}}\right) \\ \frac{b}{a}C_r\left(\frac{\dot{y}-b\dot{\epsilon}}{\dot{x}}\right) - C_f\left(\frac{\dot{y}+a\dot{\epsilon}}{\dot{x}}\right) \end{bmatrix} \quad (10)$$

$$\mathbf{g}(\dot{\mathbf{q}}, \mathbf{u}) = \begin{bmatrix} g_x \\ g_{y\epsilon} \\ g_{y\epsilon} \end{bmatrix} = \begin{bmatrix} F - F_{yf}\delta \\ F_{xf}\delta + C_f\delta \\ F_{xf}\delta + C_f\delta \end{bmatrix}. \quad (11)$$

The controlled terms, $\mathbf{g}(\dot{\mathbf{q}}, \mathbf{u})$, are determined by the control method described in the following sections. Once the entries of $\mathbf{g}(\dot{\mathbf{q}}, \mathbf{u})$ are known, (11) will be solved using (4) through (6) for the control vector, \mathbf{u} .

A. Dynamics in Terms of Sensory Information

The dynamic equations (8) are in terms of distance of the center of gravity (COG) from the road center-line. The sensors that measure the lateral deviation is not normally fixed on the vertical line through COG. Furthermore, feedback based on error measured at COG leads to bad ride comfort [2]. Hence, it is natural to describe the vehicle dynamics in terms of lateral error at the sensor, say y_s .

Assume that the sensor measuring the lateral error is at the center of the front bumper of the vehicle. Let ϵ_r be the angle between the road centerline and the vehicle

longitudinal axis in *radians*. The approximate relationship between y , y_s , and ϵ_r is

$$\epsilon_r = \frac{y_s - y}{d_s} \quad (12)$$

where d_s is the horizontal distance to the sensor from COG. Time differentiating (12), we get

$$\dot{y}_s = \dot{y} + d_s\dot{\epsilon}_r, \quad (13)$$

$$\ddot{y}_s = \ddot{y} + d_s\ddot{\epsilon}_r. \quad (14)$$

Let ϵ_d be the yaw rotation of the road center-line w. r. t. fixed earth frame, allowing us to write

$$\epsilon = \epsilon_r + \epsilon_d. \quad (15)$$

With ρ being the road curvature, it is a reasonable assumption that $\dot{\epsilon}_d = \rho\dot{x}$ [2]. Time differentiating (15), we get

$$\dot{\epsilon} = \dot{\epsilon}_r + \rho\dot{x}. \quad (16)$$

Substituting for \ddot{y} and $\ddot{\epsilon}_r$ in (14), and replacing \dot{y} by \dot{y}_s using (13), we get longitudinal and lateral dynamics in sensor space as

$$m\ddot{x} = m(\dot{y}_s - d_s\dot{\epsilon} + \rho d_s\dot{x})\dot{\epsilon} + (fk_L - k_D)\dot{x}^2 - fmg + g_x \quad (17)$$

$$\frac{m}{\xi_0}\ddot{y}_s = -\frac{m}{\xi_0}\dot{x}\dot{\epsilon} + \frac{\xi_1}{\xi_0}\dot{\epsilon} - \frac{\xi_2}{\xi_0}\left(\frac{\dot{y}_s}{\dot{x}} + \rho d_s\right) + g_{y\epsilon} \quad (18)$$

where $\xi_0 = (1 + \frac{md_s a}{I_z})$, $\xi_1 = [C_f(1 + \frac{md_s a}{I_z})(d_s - a) + C_r(1 - \frac{md_s b}{I_z})(d_s + b)]$, and $\xi_2 = [(C_f + C_r) + \frac{md_s}{I_z}(aC_f - bC_r)]$. That $\ddot{\epsilon}_d \approx 0$, and hence $\ddot{\epsilon} \approx \ddot{\epsilon}_r$, because the road curvature is piecewise continuous has also been used. Equations (17) and (18) can be rewritten as

$$m\ddot{x} = h_{s_x}(\dot{\mathbf{q}}_s) + g_x \quad (19)$$

$$\frac{m}{\xi_0}\ddot{y}_s = h_{s_{y_s}}(\dot{\mathbf{q}}_s) + g_{y\epsilon} \quad (20)$$

where $\dot{\mathbf{q}}_s = [\dot{x} \ \dot{y}_s \ \dot{\epsilon}]^T$ and $\mathbf{h}_s(\dot{\mathbf{q}}_s) = [h_{s_x}(\dot{\mathbf{q}}_s) \ h_{s_{y_s}}(\dot{\mathbf{q}}_s)]^T$ with entries defined suitably.

III. THE CONTROL APPROACH

The control objective is to simultaneously regulate the spacing error between the vehicle and the preceding vehicle, e_x , and the lateral deviation of the center of the front bumper from the road centerline, e_y . These controller tracking error definitions are consistent with previous controller designs [3]–[5]. In the sequel, subscript d is used to denote the *desired* quantities. e_x and e_y are defined as

$$e_x = x_d - x \quad (21)$$

$$e_y = y_{sd} - y_s \quad (22)$$

where $x_d = x_p - x_{spacing}$ is the difference between the longitudinal position of the preceding vehicle and the desired inter-vehicular spacing and y_{sd} is the desired lateral deviation. The relative spacing, $x_p - x$, can be obtained using radar sensors [1].

The control laws are based on a Proportional plus Derivative (PD) control scheme as

$$g_x = \hat{m}\{\ddot{x}_p + k_{vx}\dot{e}_x + k_{px}e_x + \hat{\nu}_x\} - \hat{h}_{s_x}(\dot{\mathbf{q}}_s) \quad (23)$$

$$g_{y\epsilon} = \frac{\hat{m}}{\hat{\xi}_0}\{\ddot{y}_{sd} + k_{vy}\dot{e}_y + k_{py}e_y + \hat{\nu}_y\} - \hat{h}_{s_{y_s}}(\dot{\mathbf{q}}_s) \quad (24)$$

where $\hat{(\cdot)}$ denotes the calculated (nominal) value of (\cdot) and $\hat{\nu}_x, \hat{\nu}_y$ are signals from the neural networks to counteract for modelled and unmodelled uncertainties. k_{vx}, k_{px}, k_{vy} and k_{py} are constant positive gains to be chosen by the designer.

The error rate, $\dot{e}_x = (\dot{x}_p - \dot{x}) - \dot{x}_{spacing}$ can be obtained using relative speed, $\dot{x}_p - \dot{x}$, from radar sensors [1], and $\dot{x}_{spacing}$ that may be calculated using backward difference approximations. Understandably, \ddot{x}_p , is the preceding acceleration. One simple approach to obtain \ddot{x}_p will be to apply a finite difference approximation (and preferably a low-pass filter) using \dot{x}_p that is calculated at each sampling instant as the sum of relative velocity and vehicle's velocity.

Using (19) and (23) we get

$$\hat{m}\{\ddot{x}_p + k_{vx}\dot{e}_x + k_{px}e_x + \hat{\nu}_x\} - \hat{h}_{s_x}(\dot{\mathbf{q}}_s) = m\ddot{x} - h_{s_x}(\dot{\mathbf{q}}_s)$$

or

$$\begin{aligned} \hat{m}\{\ddot{x}_p - \ddot{x} + k_{vx}\dot{e}_x + k_{px}e_x + \hat{\nu}_x\} - \hat{h}_{s_x}(\dot{\mathbf{q}}_s) \\ = (m - \hat{m})\ddot{x} - h_{s_x}(\dot{\mathbf{q}}_s) \end{aligned}$$

allowing us to write

$$\begin{aligned} \ddot{e}_x + k_{vx}\dot{e}_x + k_{px}e_x &= \left(\frac{m}{\hat{m}} - 1\right)\ddot{x} - \frac{1}{\hat{m}}\{\hat{h}_{s_x}(\dot{\mathbf{q}}_s) \\ &\quad - h_{s_x}(\dot{\mathbf{q}}_s)\} - \hat{\nu}_x \\ &= (\nu_x + \varepsilon_x) - \hat{\nu}_x \\ &= \tilde{\nu}_x. \end{aligned} \quad (25)$$

Likewise, using (20) and (24) we get

$$\begin{aligned} \ddot{e}_y + k_{vy}\dot{e}_y + k_{py}e_y &= \left(\frac{m\hat{\xi}_0}{\hat{m}\xi_0} - 1\right)\ddot{y}_s - \frac{\hat{\xi}_0}{\hat{m}}\{\hat{h}_{s_{y_s}}(\dot{\mathbf{q}}_s) \\ &\quad - h_{s_{y_s}}(\dot{\mathbf{q}}_s)\} - \hat{\nu}_y \\ &= (\nu_y + \varepsilon_y) - \hat{\nu}_y \\ &= \tilde{\nu}_y. \end{aligned} \quad (26)$$

In (25) and (26), ν_x and ν_y are the NN output signals that correspond to the ideal weights, and ε_x and ε_y with practical bounds given by $|\varepsilon_x| < \varepsilon_{xN}$, $|\varepsilon_y| < \varepsilon_{yN}$ represent the NN approximation errors.

Ideally, the goal of the neural network is to cancel off the terms in the right-hand-sides of (25) and (26) so that the errors, e_x , and e_y can asymptotically be brought to zero. Neural network is designed as separate *subnets*: viz. *x-subnet* and *y-subnet*, to separately take care of the longitudinal and lateral control problems respectively. This allows one to differently initialize the weights and independently select the design parameters to optimize the solutions to these two distinct control problems. As (25) suggests, the function to be learnt by the longitudinal subnet is a complex function of $\ddot{x}, \dot{x}, \dot{y}_s$, and \dot{e} that are hence chosen as the inputs

to the x-subnet. Likewise, $\ddot{y}_s, \dot{x}, \dot{y}_s$, and \dot{e} become the inputs to the y-subnet.

A. RBF Neural Networks

The construction of radial basis function neural networks (RBF NNs) involves three different layers: *input layer* that consists of input nodes, *hidden layer* where each neuron computes its activation using a radial basis function, and *output layer* that builds a linear weighted sum of hidden layer activations to output the response of the network. The analytic expression of the activation of a RBF with different widths that we adopt in this work can be written as

$$\psi_i(\mathbf{z}) = \exp\left(-\sum_{j=1}^f \frac{(z_j - c_{ij})^2}{2\sigma_{ij}^2}\right), \quad i = 1, 2, \dots, N \quad (27)$$

where $\mathbf{z} = [z_1, z_2, \dots, z_f]^T$ is the input vector. $c_{ij} = [c_{i1}, c_{i2}, \dots, c_{if}]^T$ and $\sigma_{ij} = [\sigma_{i1}, \sigma_{i2}, \dots, \sigma_{if}]^T$ are the center state and standard deviations of Gaussians associated with each element of input vector, respectively. N is the number of hidden-layer neurons.

B. Connection Weight Updates for Guaranteed Control Performance

We give here the NN connecting weight tuning algorithm for neural subnets in a generalized framework valid for both subnets. Subscripts are omitted for brevity. In the sequel, the notation $\|\cdot\|$ denotes Euclidean norm of a matrix vector.

The output signal, $\hat{\nu}$, from a three-layered RBF NN can be written as

$$\hat{\nu} = \hat{\mathbf{w}}^T \cdot \boldsymbol{\psi}(\mathbf{z}) \quad (28)$$

where $\boldsymbol{\psi}, \hat{\mathbf{w}} \in \mathfrak{R}^N$ are the vector of activations of hidden-layer neurons and the vector of current values of connecting weights between the hidden-layer and the single (in this example) output node, respectively. Expanding (28) into a Taylor series yields

$$\nu - \hat{\nu} = (\mathbf{w} - \hat{\mathbf{w}})^T \cdot \boldsymbol{\psi} + \zeta \quad (29)$$

where ζ ($|\zeta| < \zeta_N$) represents neglected higher order terms. Combining (25) (or (26)) and (29), we have

$$\tilde{\nu} = \tilde{\mathbf{w}}^T \boldsymbol{\psi} + \varepsilon + \zeta \quad (30)$$

where $\tilde{\mathbf{w}} = \mathbf{w} - \hat{\mathbf{w}}$ is the weight estimation error with \mathbf{w} ($\|\mathbf{w}\| \leq w_{\max}$) being ideal weights.

Rewriting the terms in equation (25) (or (26)), yields

$$\dot{e} = A e + B \tilde{\nu} \quad (31)$$

where

$$e = \begin{bmatrix} e \\ \dot{e} \end{bmatrix}, \quad A = \begin{bmatrix} 0 & 1 \\ -k_p & -k_v \end{bmatrix}, \quad B = \begin{bmatrix} 0 \\ 1 \end{bmatrix}.$$

Note that, if the desired spacing, $x_{spacing}$, is a constant, $\dot{e}_x (= \dot{x}_p - \dot{x})$ turns out to be the velocity error. Define the error signal to the NN, r , as

$$r = e + \dot{e} = C e \quad (32)$$

where $C = [1 \quad 1]$. Equations (31) and (32) give the state-space representation of error dynamics. Let s be the Laplace operator. Simple computations prove that whenever $k_v \geq 1$, $\text{Re } T(s - \varrho)$ of the transfer function of error dynamics $T(s)$ is non-negative, for a real $\varrho > 0$, if the following condition holds

$$\sigma - \varrho > - \left[\frac{(k_v + 1)(\sigma - \varrho)^2 + (k_v - 1)\omega^2 + k_p}{(\sigma - \varrho)^2 + \omega^2 + k_v + k_p} \right].$$

This confirms that $T(s - \varrho)$ is positive real for some real $\varrho > 0$, and hence $T(s)$ is strictly positive real.

Let the NN weight tuning be provided by

$$\dot{\hat{w}} = \eta r \psi - \kappa \|e\| \hat{w} \quad (33)$$

where $\eta > 0$ is any constant scalar parameter and $\kappa > 0$ a design parameter. Then, the error and error rate, e , is bounded and the NN weight convergence is guaranteed with practical bounds.

In order to prove the above results, define the Lyapunov function candidate as

$$L(e, \tilde{w}) = e^T P e + \frac{1}{\eta} \tilde{w}^T \tilde{w} \quad (34)$$

where P is a positive definite solution of the Lyapunov equation $A^T P + P A + Q = 0$, for any positive definite matrix Q . Differentiating (34) yields

$$\dot{L} = \dot{e}^T P e + e^T P \dot{e} + \frac{2}{\eta} \dot{\hat{w}}^T \tilde{w}.$$

Substitution for \dot{e} from (31) and rearranging yields

$$\dot{L} = e^T (A^T P + P A) e + 2e^T (P B) \tilde{v} + \frac{2}{\eta} \dot{\hat{w}}^T \tilde{w}.$$

From Kalman-Yakubovich-Popov (KYP) lemma [8], when the transfer function is made strictly positive real, for the system described by (31) and (32) there exist two positive-definite symmetric matrices P and Q , satisfying KYP system

$$A^T P + P A + Q = 0, \quad P B = C^T.$$

Now

$$\dot{L} = -e^T Q e + 2e^T C^T \tilde{v} + \frac{2}{\eta} \dot{\hat{w}}^T \tilde{w}.$$

Substitution for \tilde{v} from (30) gives

$$\begin{aligned} \dot{L} &= -e^T Q e + 2(Ce)^T (\tilde{w}^T \psi + \varepsilon + \zeta) + \frac{2}{\eta} \dot{\hat{w}}^T \tilde{w} \\ &= -e^T Q e + 2r \tilde{w}^T \psi + 2(Ce)^T (\varepsilon + \zeta) + \frac{2}{\eta} \dot{\hat{w}}^T \tilde{w}. \end{aligned}$$

Using the property $\tilde{w}^T \psi = \psi^T \tilde{w}$ for $\tilde{w}, \psi \in \mathfrak{R}^N$ and shuffling the terms, we get

$$\dot{L} = -e^T Q e + 2(Ce)^T (\varepsilon + \zeta) + \frac{2}{\eta} \dot{\hat{w}}^T \tilde{w} + 2r \psi^T \tilde{w}.$$

Since $\dot{\hat{w}} = -\dot{\hat{w}}$, with tuning rule (33)

$$\begin{aligned} \dot{L} &= -e^T Q e + 2(Ce)^T (\varepsilon + \zeta) \\ &\quad + 2 \frac{\kappa}{\eta} \|e\| \|\hat{w}\|^T (w - \hat{w}). \end{aligned}$$

Since $a^T (b - a) \leq \|a\| \|b\| - \|a\|^2$ for any $a, b \in \mathfrak{R}^n$, it follows that

$$\hat{w}^T (w - \hat{w}) \leq \|\hat{w}\| \|w\| - \|\hat{w}\|^2. \quad (35)$$

And also

$$\begin{aligned} -e^T Q e + 2(Ce)^T (\varepsilon + \zeta) \\ \leq -Q_{\min} \|e\|^2 + 2\sqrt{2}(\varepsilon_N + \zeta_N) \|e\| \end{aligned} \quad (36)$$

where Q_{\min} is the minimum singular value of Q . Because of the inequalities (35) and (36), there results

$$\begin{aligned} \dot{L} &\leq -Q_{\min} \|e\|^2 + 2 \frac{\kappa}{\eta} \|e\| \|\hat{w}\| (w_{\max} - \|\hat{w}\|) \\ &\quad + 2\sqrt{2}(\varepsilon_N + \zeta_N) \|e\| \\ &= -\|e\| [Q_{\min} \|e\| + 2 \frac{\kappa}{\eta} \|\hat{w}\| (\|\hat{w}\| - w_{\max}) \\ &\quad - 2\sqrt{2}(\varepsilon_N + \zeta_N)] \end{aligned}$$

which is negative if the term within braces (TWB) is positive. We can write

$$\begin{aligned} \text{TWB} &= 2 \frac{\kappa}{\eta} (\|\hat{w}\| - w_{\max}/2)^2 - \kappa w_{\max}^2 / 2\eta \\ &\quad + Q_{\min} \|e\| - 2\sqrt{2}(\varepsilon_N + \zeta_N) \end{aligned}$$

which is guaranteed to be positive as long as either

$$\|e\| > \frac{\kappa w_{\max}^2 / 2\eta + 2\sqrt{2}(\varepsilon_N + \zeta_N)}{Q_{\min}}$$

or

$$\|\hat{w}\| > w_{\max}/2 + \sqrt{w_{\max}^2/4 + \sqrt{2}\eta(\varepsilon_N + \zeta_N)/\kappa}.$$

Therefore, \dot{L} is negative outside a compact set, and weight and error convergence is guaranteed.

C. Calculating $u = [F \delta]^T$

According to (11), it follows that

$$g_x = F + \hat{C}_f \beta_1 \delta \quad (37)$$

$$g_{y\epsilon} = (F - \beta_2) \delta + \hat{C}_f \delta \quad (38)$$

where $\beta_1 = \frac{\dot{y} + \hat{a}\dot{e}}{\hat{x}}$ and $\beta_2 = \hat{f}_{\frac{\hat{b}}{\hat{a} + \hat{b}}} (\hat{m}g - \hat{k}_L \dot{x}^2)$. It was assumed that $\delta^2 = 0$. Recall that (\cdot) denotes the nominal value of (\cdot) and that $\hat{a} + \hat{b}$ is vehicle's wheel-base.

From (37) and (38) we get

$$g_{y\epsilon} = (g_x - \hat{C}_f \beta_1 \delta) \delta + (\hat{C}_f - \beta_2) \delta$$

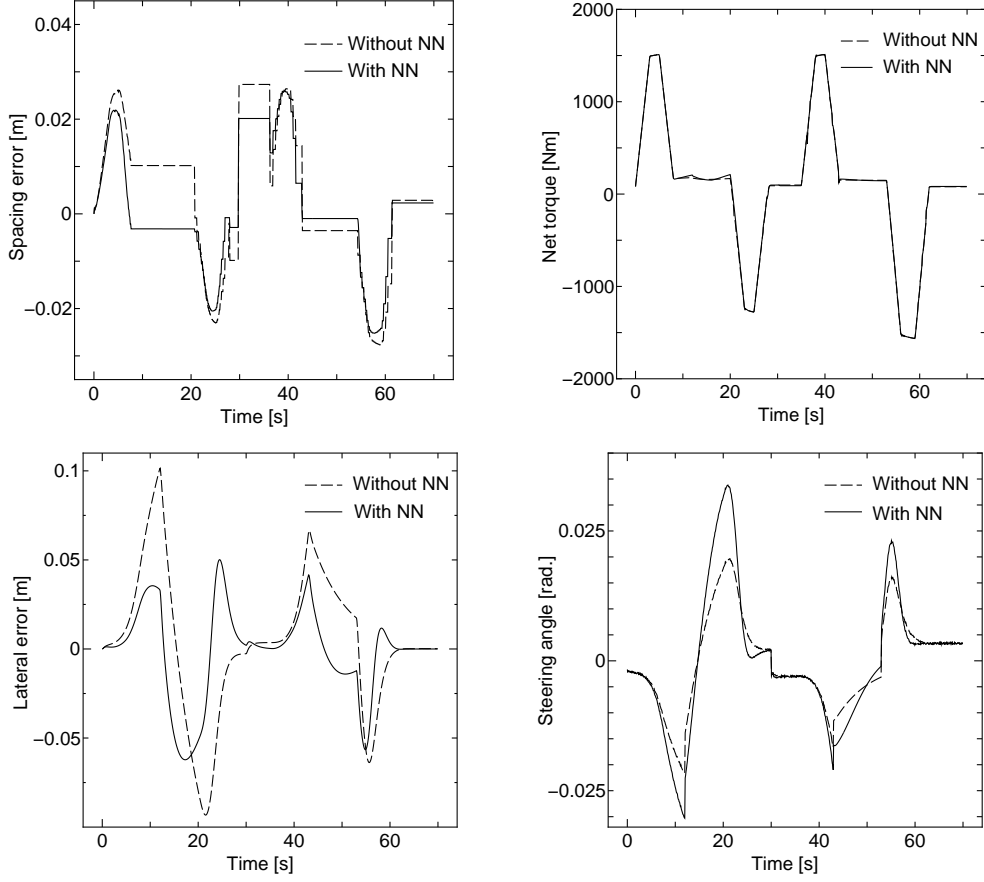


Fig. 2. Simulation results.

or

$$a_0\delta^2 + b_0\delta + c_0 = 0$$

where $a_0 = \hat{C}_f\beta_1$, $b_0 = \beta_2 - g_x - \hat{C}_f$, and $c_0 = g_y\epsilon$. This gives

$$\delta = \begin{cases} \frac{-b_0 - \sqrt{b_0^2 - 4a_0c_0}}{2a_0} & \text{if } a_0 \neq 0 \\ -\frac{c_0}{b_0} & \text{if } a_0 = 0 \end{cases} \quad (39)$$

Net force, F , is now obtained using (37) and (39).

IV. SIMULATIONS

Simulation tests are performed using the original unsimplified model. $x_{spacing}$ is chosen to be constant, and $y_{sd} = \dot{y}_{sd} = \ddot{y}_{sd} = 0$. Total mass of the vehicle, m , is taken to be $m = \hat{m} + 300$ kg for 4×75 kg passengers on board. Coherently, $I_z = \frac{m}{\hat{m}} \hat{I}_z$. The cornering stiffnesses are $C_f = 0.75 \hat{C}_f$, $C_r = 0.75 \hat{C}_r$; position of center-of-gravity, $a = 1.1 \hat{a}$; aerodynamic parameters, $k_D = 1.1 \hat{k}_D$, $k_L = 1.1 \hat{k}_L$; rolling resistance, $f = 0.9 \hat{f}$.

The practical bounds for acceleration capability of the vehicle is assumed to be given by $110250.0/m\dot{x}$ ms^{-2} for $\dot{x} \geq 12.5$ ms^{-1} (maximum engine power of 150 PS) and 3 ms^{-2} otherwise. PD control law parameters are selected as $k_{vx} = k_{vy} = 10$, $k_{px} = k_{py} = 15$.

Input vectors to the longitudinal- x and lateral- y neural subnets respectively are $\mathbf{z}_x = [\ddot{x} \dot{x} \dot{y}_s \dot{\epsilon}]^T$ and $\mathbf{z}_y = [\ddot{y}_s \dot{x} \dot{y}_s \dot{\epsilon}]^T$. Except for c_{i2} 's, which associate with longitudinal velocity, \dot{x} , center states are set in the range $[-2, 2]$ for both subnets. c_{i2} 's are set in the range $[5, 30]$. For the same reason, σ_{i2} 's are differently set at $8/\sqrt{2}$ while other standard deviations are set at $2/\sqrt{2}$. Adaptation law parameters are selected as $\eta_x = 5$, $\eta_y = 50$, $\kappa_x = \kappa_y = 0.001$. Each subnet has 7 hidden neurons and the connecting weights are all initialized at zero.

Controller performance and control inputs are depicted in Fig. 2. Fig. 3 gives the simulation profiles.

V. CONCLUSIONS

This paper has presented a novel control approach for combined longitudinal and lateral vehicle control for IVHS. The controller has also been tested and verified via computer simulations under severe acceleration conditions and model uncertainties using a dynamic model that has strong nonlinearity and coupling terms. Weights of the neural modules can simply be initialized at zero and be adapted completely online without needing any off-line training phase. Stability has been guaranteed based on a Lyapunov approach.

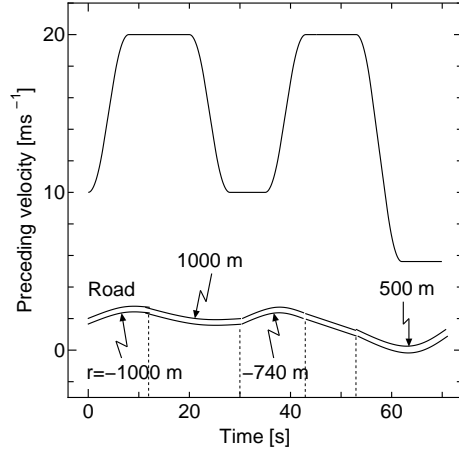


Fig. 3. Simulation profiles.

TABLE I
PARAMETERS (NOMINAL) OF THE VEHICLE SYSTEM

Description	Value
\hat{m} Total mass of the vehicle	1760 kg
\hat{I}_z Yaw inertia	3332 kgm ²
\hat{f} Rolling friction coefficient	0.02
\hat{a} Distance–front wheel to CG	1.193 m
L Wheel-base ($\hat{a} + \hat{b}$)	2.78 m
\hat{d}_s Distance–front bumper to CG	2.103 m
\hat{C}_f Cornering Stiffness–front	131391 N/rad
\hat{C}_r Cornering Stiffness–rear	115669 N/rad
\hat{k}_L Aerodynamics–lift parameter	0.008 Ns ² m ⁻²
\hat{k}_D Aerodynamics–drag parameter	0.49 Ns ² m ⁻²

REFERENCES

- [1] J. Mar and F. J. Lin, “An ANFIS Controller for the Car-following Collision Prevention System,” *IEEE Trans. on Vehicular Technology*, Vol. 50, No. 4, pp. 1106–1113, 2001.
- [2] P. S. Hingwe, “Robustness and Performance Issues in the Lateral Control of Vehicles in Automated Highway Systems”, Ph.D. Dissertation, Univ. California at Berkeley, 1997.
- [3] J. K. Hedrick, D. McMahon, and V. Narendran, “Longitudinal Vehicle Controller Design for IVHS Systems”, *Procs. of the American Control Conference*, pp. 3107–3112, 1991.
- [4] E. H. M. Kim and J. K. Hedrick, “Lateral and Longitudinal Vehicle Control Coupling for automated Vehicle Operation”, *Procs. of the American Control Conference*, pp. 3676–3680, 1999.
- [5] H. Pham, J. K. Hedrick, and M. Tomizuka, “Combined Lateral and Longitudinal Control of Vehicles for IVHS”, in *Procs. of the American Control Conference*, pp. 1205–1206, 1994.
- [6] H. Lee and M. Tomizuka, “Coordinated Longitudinal and Lateral Motion Control of Vehicles for IVHS,” *ASME Journal of Systems, Measurement, and Control*, Vol. 123, pp. 535–543, 2001.
- [7] E. Bakker, L. Nyborg, and H. B. Pacejka, “A New Tire Model with an Application in Vehicle Dynamics Studies,” *SAE Transactions, Journal of Passenger Cars*, Vol. 98, paper no. 890087, 1989.
- [8] M. Vidyasagar, *Nonlinear Systems Analysis—2nd Edition*. Englewood Cliffs, NJ: Prentice-Hall, 1993.